Available online at www.HEFJournal.org

Journal of
Human, Earth, and Future

ISSN: 2785-2997

Vol. 7, No. 1, March, 2026

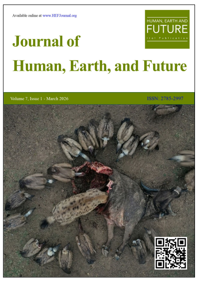

Development of Flood Risk Management Modeling Due to the Regional Spatial

Yuli Astuti [1], Pitojo Tri Juwono [1], Lily M. Limantara [1*], Riyanto Haribowo [1]

[1] *Department of Water Resources Engineering, Faculty of Engineering, University of Brawijaya, Malang, Indonesia.*

Received 07 October 2025; Revised 26 December 2025; Accepted 11 January 2026; Published 01 March 2026

Abstract

This study examines flood risk conditions in the Juwana River watershed, Central Java, through the development of a quantitative framework that incorporates destructive power (H), vulnerability (V), and institutional capacity (C). Conceptually, the relationship among these components is represented by the fundamental risk formulation R = H x V/C. A GIS-based Multi-Criteria Risk Assessment (MCRA) approach was applied to integrate the hazard (H), capacity (C), and vulnerability (V) indicators within a spatial analytical environment. This conceptual model was subsequently calibrated through a non-linear regression procedure, resulting in the empirical formulation $R = 0.695 \cdot H^{0.032} \cdot C^{0.233} \cdot V^{0.711}$. The analytical results demonstrate that flood risk is influenced by the combined effects of hydrodynamic characteristics and socio-institutional conditions. Areas undergoing rapid land-use transformation tend to exhibit higher levels of vulnerability due to increased exposure of populations and assets, whereas stronger institutional capacity is associated with reduced risk through enhanced mitigation, preparedness, and emergency response mechanisms. The analytical framework provides insights that may support informed decision-making in prioritizing interventions, allocating resources, and strengthening regional flood management practices.

Keywords: Flood Modelling; Flood Risk; Flood Management; Regional Spatial.

1. Introduction

Urban expansion is increasingly altering flood-prone landscapes, intensifying the challenges of urban flood disasters. Flood risk management provides a scientific foundation for present and future urban flood mitigation and preparedness [1]. This process involves hazard identification, exposure and vulnerability assessment, and comprehensive risk evaluation as the basis for spatially informed mitigation planning and decision-making.

In recent years, the coupling of GIS-based spatial analysis with two-dimensional (2D) hydrodynamic modelling has significantly improved the accuracy of flood hazard mapping and the reliability of risk assessment in urban environments [2–6]. These techniques enable the simulation of inundation dynamics such as flow velocity, flood depth, and spatial extent providing a more realistic representation of hazard distribution for urban flood management. However, conventional flood risk assessments often overlook the destructive power of floodwaters, including flow momentum, debris transport, and potential structural damage, which represent critical gaps in current flood risk evaluation frameworks [7-9]. Ignoring destructive power can lead to under-estimation of physical and economic impacts and may limit the effectiveness of mitigation strategies.

* Corresponding author: lilymont@ub.ac.id; yuli.astuti@agrinaspalma.id

https://doi.org/10.28991/HEF-2026-07-01-011

Several studies have applied univariate indicators, such as flood depth [10], or population exposure, to represent flood risk, whereas others employ multivariate models that combine hydrological, socio-economic, and environmental factors. As emphasized by Apel et al. [7] and Pradhan et al. [9], flood impacts extend beyond physical and economic losses to include social and psychological effects, such as fatalities and emotional trauma. Consequently, recent studies have incorporated social and environmental vulnerability indicators, such as population density, poverty level, and access to emergency facilities, into GIS and machine learning frameworks to better quantify and visualize spatial risk patterns [11-15]. Integrating destructive power alongside these conventional indicators allows for a more comprehensive assessment of flood impacts and supports evidence-based decision-making for adaptive urban planning.

Methodologically, various frameworks have been developed, including statistical analysis based on historical data [16], index-based systems [17], scenario simulation [18], and GIS-based spatial modelling [19]. While statistical and scenario-based analyses depend largely on observed or simulated hydrological data, index and GIS-based approaches allow the integration of multi-dimensional indicators, facilitating comprehensive spatial risk mapping across regional and urban scales [20].

The theoretical foundation of this study is grounded in the integrative flood risk paradigm, which conceptualizes risk as a function of hazard intensity, exposure characteristics, and socio-economic vulnerability. This paradigm is consistent with international frameworks established by UNDRR (United Nation Office for Disaster Risk Reduction), which describe flood risk as the interaction between physical flood processes and the susceptibility and adaptive capacity of exposed systems. In this framework, hazard is defined not only by inundation depth and spatial extent but also by the destructive power of floodwaters, which reflects combined influences of flow velocity, momentum, and potential structural impact. Vulnerability is treated as a multidimensional construct encompassing demographic, socio-economic, and environmental determinants of harm, while institutional capacity is incorporated as a moderating factor that can reduce or intensify risk by shaping preparedness, mitigation, and emergency response performance. By adopting this theoretical basis, the study operationalizes risk through both a conceptual formulation ($R = H \times V / C$) and an empirically calibrated model, ensuring coherence between the theoretical assumptions and the methodological procedures employed.

Within the context of land-use dynamics, the Juwana River System exemplifies the increasing complexity of flood risk associated with spatial transformation. Areas that once served as natural retention wetlands have been converted into agricultural, residential, and industrial zones. These spatial transitions, combined with increasing population density, have intensified potential physical damage and socio-economic losses, thereby complicated flood risk management and necessitating an integrated, multidisciplinary approach.

A multidisciplinary framework integrating hydrodynamic modelling, spatial planning analysis, socio-economic vulnerability assessment, destructive power evaluation, and climate scenario projections is essential to ensure comprehensive and sustainable flood risk management. Such an approach not only strengthens the analytical foundation for flood risk evaluation but also enhances policy relevance and supports adaptive spatial planning in flood-prone regions [19–20].

The remainder of this manuscript is arranged as follows. Section 2 elaborates the conceptual framework and methodological approach. Section 3 presents the results and spatial analyses. Section 4 discusses the broader implications of the findings. Section 5 concludes the study and outlines potential avenues for future work.

2. Materials and Methods

In this study, flood risk management was assessed through an integrated approach combining hydrodynamic simulation, spatial analysis, and socio-economic vulnerability evaluation. The methodology was structured into four main stages:

(1) Data collection and preprocessing, including topographic, rainfall, land use, and population datasets;

(2) Hydrodynamic modelling using a two-dimensional (2D) model to simulate flood depth and flow velocity

(3) Spatial analysis within a GIS environment to derive hazard indicators; and

(4) Integration of hazard, exposure, and vulnerability parameters to generate the flood risk index.

This approach responds to the data limitations commonly faced in developing countries by utilizing freely available datasets (e.g., DEM from SRTM) and open-source GIS tools. Socio economic variables such as population density and income level were incorporated to ensure that flood risk management strategies reflect both technical and community-based resilience aspects.

2.1. Study Location

This research is conducted in Juana River region, specifically in the Juana Watershed (Figure 1), in Pati and Kudus Regencies. There are 11 sub-watersheds that are Gembong, Juana 1a, Juana1b, Juana 1c, Juana 1d, Juana 2a, Juana 2b, Juana 2c, Juana 3a, Juana3b, and Logung.

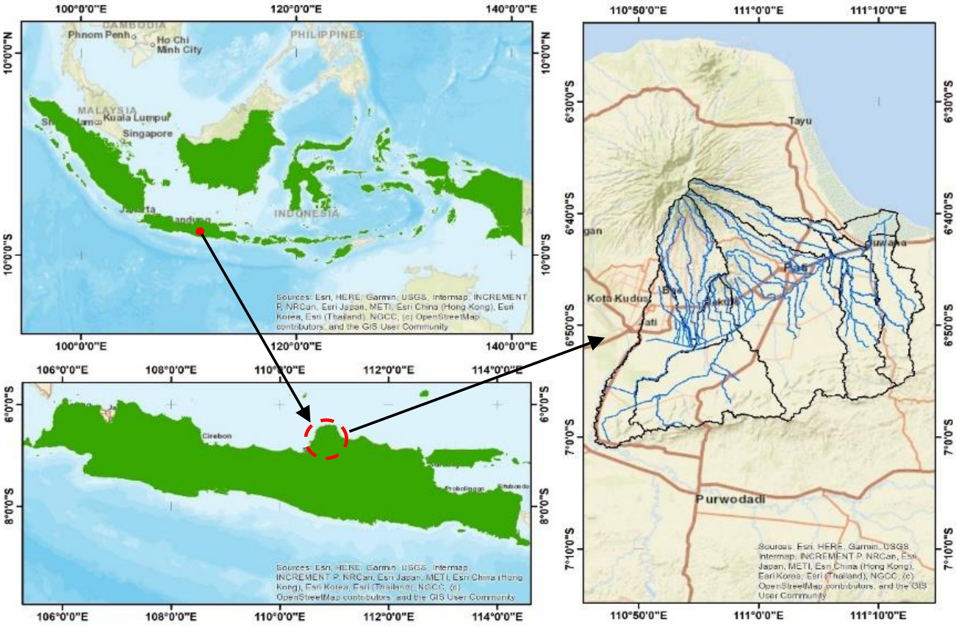

Figure 1. Research Location

2.2. Data Collection and Model Development

The data used in this study were derived from multiple sources, combining spatial, environmental, hydrological, and socio-economic datasets to support a comprehensive flood risk modelling approach. The integration of spatial planning layers (RTRW) with environmental and hazard data enabled the development of a robust framework for evaluating flood risk within the context of land-use allocation and regional planning.

(a) Spatial and Environmental Data

Spatial planning data, including land-use zones, settlement hierarchies, and infrastructure networks, were obtained from the official *Regional Spatial Plan (RTRW)* of the study area. Forest cover, vegetation indices, and topographic information were extracted from remote sensing datasets, including *Landsat 8 OLI/TIRS*, *Sentinel-2 MSI*, and *MODIS NDVI composites* (2019–2024). Digital Elevation Models (DEM) from *SRTM (30 m resolution)* were used to derive slope, flow direction, and watershed boundaries. These datasets were processed and standardized within a GIS environment for subsequent spatial overlay analysis.

(b) Hydrological and Meteorological Data

Hydrological parameters including rainfall intensity, flow discharge, and river network configuration were obtained from the *Indonesian Agency for Meteorology, Climatology, and Geophysics (BMKG)* and the *Ministry of Public Works and Housing (PUPR)*. Daily rainfall data (2010–2024) from at least five monitoring stations were analysed using frequency distribution methods to estimate design rainfall for different return periods (2-, 5-, 10-, 25-, and 50-year). River discharge data were used to calibrate and validate the hydrological simulation model (HEC-HMS), while hydraulic behaviour within the floodplain was analysed using HEC-RAS 2D.

(c) Socio-Economic and Exposure Data

Population density, building footprints, and critical infrastructure were derived from World Pop, *OpenStreetMap*, and regional statistical data (*BPS*). These layers were used to quantify vulnerability indicators, allowing risk to be evaluated not only by physical inundation but also by potential socio-economic losses.

(d) Model Development

A GIS based Multi-Criteria Risk Assessment (MCRA) approach was applied to integrate hazard (H), capacity (C), and vulnerability (V) indicators. Each factor was standardized using a fuzzy membership function, and weights were assigned using the Analytic Hierarchy Process (AHP) based on expert judgement and literature derived significance levels.

Figure 2 shows the flowchart of the research methodology through which the objectives of this study were achieved.

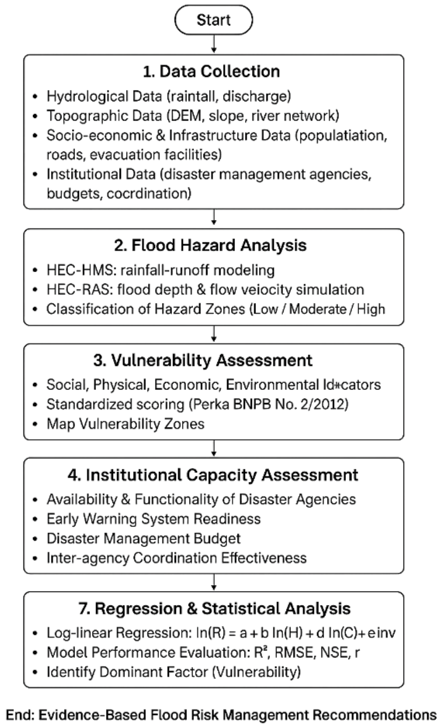

Figure 2. Flood Risk Assessment and Modelling Framework

3. Results

In order to support the planning of effective flood risk mitigation, the result of spatial analysis is used for analysing the area that is included in each risk class that is low, moderate, and high. This approach is possible to quantitatively identification to the distribution of flood risk in the study area, so it makes easy the prioritization of mitigation action and the allocation of water resources is right on target.

3.1. Determination of Flood Depth Hazard Classification with Probability

Flood hazard classification was performed using spatial analysis, dividing the area into three hazard classes: low, moderate, and high. The assessment considered flood frequency probability, rainfall intensity, topography, and drainage system availability. Hydrological and hydraulic modelling was conducted using HEC-HMS and HEC-RAS, and flood depth hazard maps were generated for 2020, 2025, 2045, and 2070. Figure 3 presents the flood depth hazard map for 2025.

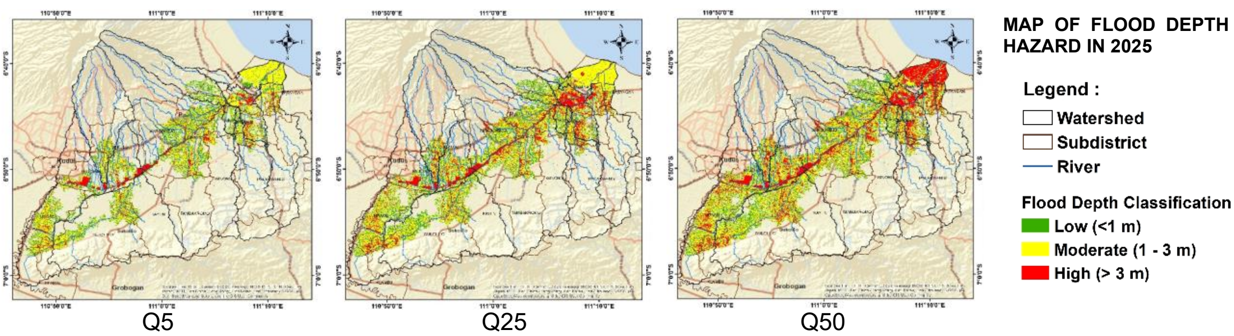

Figure 3. Map of Flood Depth Hazard 2025 for Some Return-Periods

3.2. Classification of Flood Destructive Power Hazard (H)

Flood destructive power hazard was analysed based on the combination of inundation depth and flow velocity, consistent with FEMA guidelines. Flood depth and velocity data were obtained from HEC-RAS hydrodynamic simulations. Integrating HEC-RAS results with spatial analysis improved the accuracy and relevance of flood risk information, supporting informed decision-making for disaster risk reduction and regional resilience enhancement. Flood destructive maps were produced for 2020, 2025, 2045, and 2070 (Figure 4).

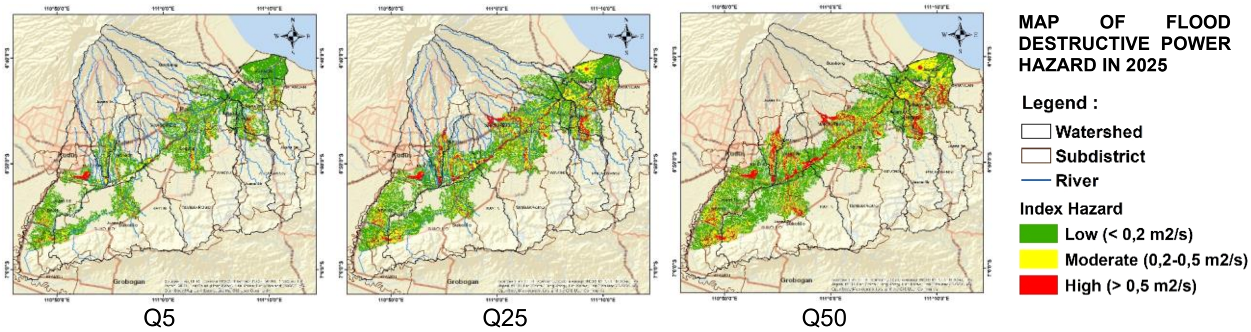

Figure 4. Map of Flood Destructive Power Hazard 2025 for Some Return-Periods

3.3. Analysis of Vulnerability (V)

Regional vulnerability was evaluated based on four components: social, physical, economic, and environmental. Specific indicators included population density, infrastructure quality, poverty rate, and ecosystem condition. Standardized vulnerability scores were calculated following BNPB guidelines (Perka BNPB No. 2, 2012). Flood vulnerability maps were developed for 2020, 2025, 2045, and 2070 (Figure 5).

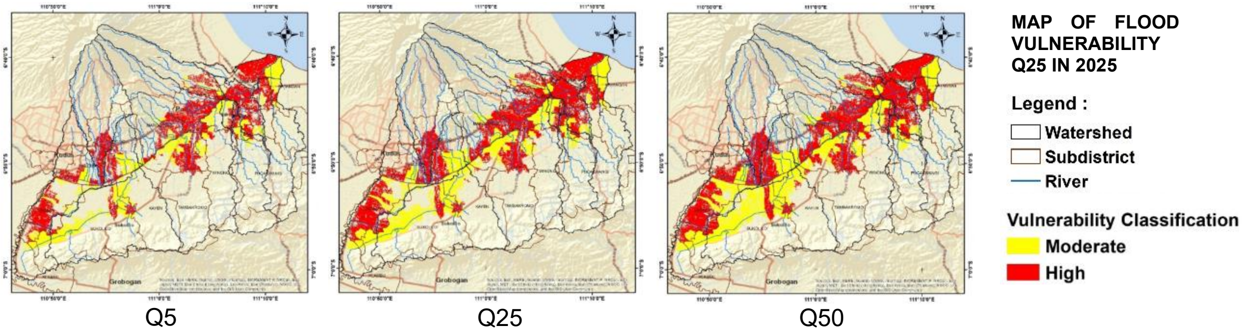

Figure 5. Map of Vulnerability to Flood 2025 for Some Return-Periods

3.4. Assessment of Institution Capacity (C)

The institution capacity in facing the flood risk is assumed on the high level, based on the report of BNPB, 2024. This assumption involves the ability of local institution in planning, response, disaster mitigation, and the availability of human resources and supporting infrastructure. The assessment of the capacity is the limitation of this research, and it is used as the permanent parameter in the risk analysis.

3.5. Assessment of Flood Risk (R)

Flood risk was assessed using the formulation $R = H (V/C)$ to identify high risk areas for targeted mitigation. Risk maps were produced for 2020, 2025, 2045, and 2070. Figure 6 shows flood risk based on depth hazard, and Figure 7 on destructive power hazard for 2025, providing a spatial overview of potential flood impacts.

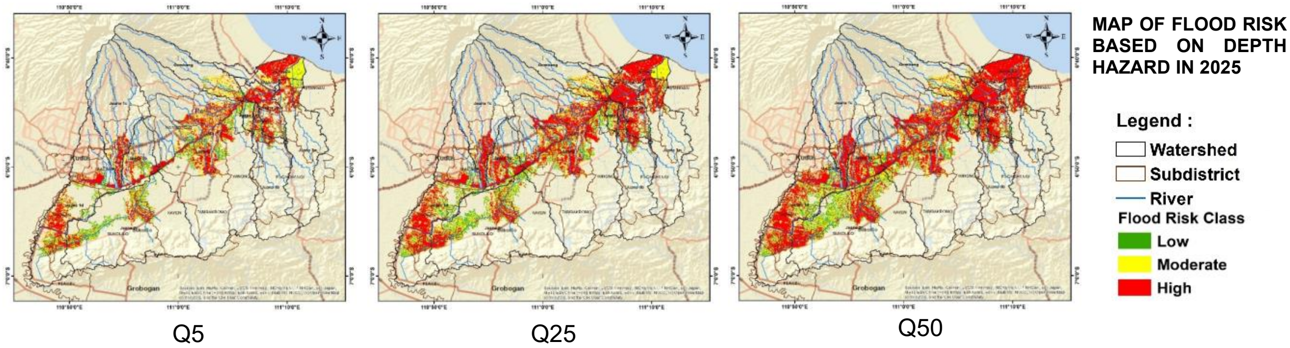

Figure 6. Map of Flood Risk Based on Depth Hazard 2025 for Some Return-Periods

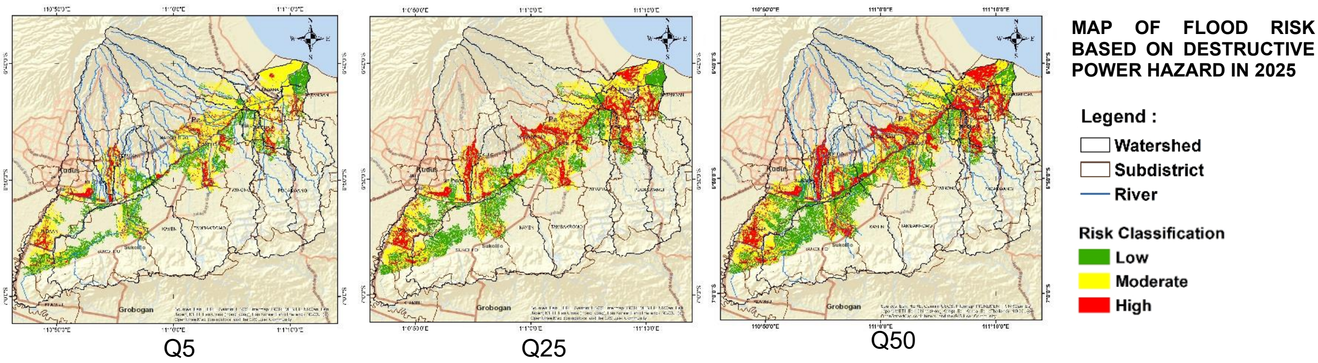

Figure 7. Map of Flood Risk Based on Destructive Power Hazard 2025 for Some Return-Periods

3.6. Quantitative Analysis for Risk Assessment Classification

A quantitative analysis was conducted using Geographic Information System (GIS) techniques to classify and evaluate areas according to their respective risk levels low, moderate, and high. This analysis supports effective flood risk mitigation planning. The GIS based spatial analysis was applied to calculate the total area within each risk class, enabling precise quantification of flood affected zones.

3.7. Flood Risk Modelling

Initially, a flood risk map is generated by integrating hazard, vulnerability, and capacity data using GIS based spatial analysis. Each spatial unit, such as a grid or polygon, is then classified into a specific risk class according to its calculated risk index. Following classification, the area corresponding to each risk class is determined by summing the spatial units within each category. The resulting data are subsequently presented in a matrix or risk distribution table, illustrating the area associated with each risk class. Table 1 presents the flood risk assessment matrix for both flood depth hazard and destructive power hazard for the Q5 discharge (5-year return period) in 2020.

Table 1. Matrix of Flood Risk Modelling Due to Q_5 on 2020

			PRESENT				MODIFIED MODEL			
River Basin		Risk Index	R = H (V/C)	H depth based on simulated flood	C (Capacity)	V (vulnerability)	R =Hx (V/C)	H destructive power based on simulated flood	C (Capacity)	V (vulnerability)
1	Gembong	Low	1.407	6.892	0.000	0.000	2.639	10.597	0.000	0.000
		Moderate	7.019	5.054	0.000	3.363	9.331	0.240	0.000	3.363
		High	4.455	0.937	12.850	9.487	0.880	0.104	12.850	9.487
2	Juana 1a	Low	1.269	2.163	0.000	0.000	3.669	5.957	0.000	0.000
		Moderate	3.207	3.567	0.000	4.747	2.866	0.280	0.000	4.747
		High	2.924	1.676	7.391	2.644	0.856	0.117	7.391	2.644
3	Juana 1b	Low	1.509	2.485	0.000	0.000	2.923	6.671	0.000	0.000
		Moderate	3.663	5.372	0.000	5.487	3.874	2.456	0.000	5.487
		High	4.960	2.273	10.094	4.607	3.297	0.532	10.094	4.607
4	Juana 1c	Low		3.790	0.000	0.000		7.469	0.000	0.000
		Moderate	3.788	7.258	0.000	0.000	5.947	4.613	0.000	0.000
		High	10.679	3.420	14.428	14.428	8.481	2.015	14.428	14.428
5	Juana 1d	Low	8.501	18.786	0.000	0.000	18.048	63.121	0.000	0.000
		Moderate	22.484	29.407	0.000	26.238	27.906	12.697	0.000	26.238
		High	30.757	13.587	61.575	35.337	15.621	3.661	61.575	35.337
6	Juana 2a	Low	0.365	2.973	0.000	0.000	6.848	23.864	0.000	0.000
		Moderate	9.361	23.266	0.000	7.306	14.515	1.568	0.000	7.306
		High	17.797	1.349	27.514	20.208	6.151	0.313	27.514	20.208

7	Juana 2b	Low	1.288	5.665	0.000	0.000	2.931	21.190	0.000	0.000
		Moderate	6.763	11.743	0.000	4.833	13.345	4.198	0.000	4.833
		High	22.121	12.773	30.064	25.231	13.788	2.196	30.064	25.231
8	Juana 2c	Low	14.930	18.646	0.000	0.000	30.424	47.261	0.000	0.000
		Moderate	24.924	25.975	0.000	41.387	15.727	5.716	0.000	41.387
		High	11.147	6.381	50.930	9.543	4.779	1.086	50.930	9.543
9	Juana 3a	Low	1.397	3.280	0.000	0.000	3.108	11.330	0.000	0.000
		Moderate	5.467	8.013	0.000	5.902	6.924	2.809	0.000	5.902
		High	9.200	4.771	16.016	10.114	5.984	1.100	16.016	10.114
10	Juana 3b	Low	2.824	6.841	0.000	0.000	5.715	17.432	0.000	0.000
		Moderate	8.691	9.088	0.000	11.516	11.075	3.598	0.000	11.516
		High	10.983	6.570	22.468	10.952	5.678	0.874	22.468	10.952
11	Logung	Low	9.123	27.928	0.000	0.000	20.541	66.857	0.000	0.000
		Moderate	34.277	46.958	0.000	34.554	43.925	10.885	0.000	34.554
		High	52.542	21.068	95.686	61.132	31.220	3.214	95.686	61.132

3.8. Model Evaluation

To evaluate how far the regression model is able to present the relation between independent and dependent variables, there is carried out the statistical analysis by determination coefficient (R^2). This evaluation is one of the main techniques in regression analysis because it gives the quantitative size to the proportional variation of dependent variable that can be explained by the independent variable in the model that is used.

In this study, the value of R^2 is used for comparing the contribution level between the parameter of flood depth (H) and the parameter of flood destructive power ($H_{destructive\ power}$) in explaining the frequency of actual flood on the different year.

Table 2. Determination Coefficient of Flood Risk

No.	Year	Probability Flood	R^2	
			H depth	H damage
1	2020	Q_5	0.92	0.587
2		Q_{25}	0.87	0.679
3		Q_{50}	0.96	0.798
4	2025	Q_5	0.90	0.593
5		Q_{25}	0.95	0.702
6		Q_{50}	0.97	0.784
7	2045	Q_5	0.94	0.364
8		Q_{25}	0.96	0.432
9		Q_{50}	0.96	0.503
10	2070	Q_5	0.89	0.456
11		Q_{25}	0.93	0.565
12		Q_{50}	0.98	0.630

Table 2 presents the statistical analysis result that is determination coefficient (R^2) for 2 main parameters: flood depth (H_{depth}) and flood destructive power ($H_{destructive\ power}$) that is analysed for some quantile scenarios (Q_5, Q_{25}, and Q_{50}) in the different time periods that are 2020, 2025, 2045, and 2070.

Flood depth (H_{depth}) consistently exhibited high R^2 values (0.868–0.981) across quantile scenarios (Q5, Q25, Q50) for 2020–2070, indicating strong explanatory power of the input parameters. In contrast, R^2 for flood destructive power ranged from 0.431 to 0.798, reflecting the additional complexity influenced by structural characteristics, socioeconomic factors, and infrastructure resilience not fully captured by the model.

The performance of the flood risk models was evaluated using determination coefficient (R^2), Root Mean Square Error (RMSE), Nash–Sutcliffe Efficiency (NSE), and correlation coefficient (r). RMSE, NSE, and r were used to quantify prediction accuracy. The result of RMSE and NSE for the flood modelling are as follow: the RMSE is 12.009

and NSE is 0.601; the correlation is 0.629 and the R^2 is 0.396. The RMSE is 12.009, it indicates that the deviation average between model prediction result to the actual data is in the range of 12 units. This value gives the quantitative illustration about the size of prediction error which the smaller RMSE indicates the model is getting accurate.

The NSE is 0.601, it indicates that the model has good enough ability in explaining the variability of data. The value of NSE is between −∞-\nifty−∞ until 1, If the value is close to 1, it indicates that the model performance is very good. In this context, the value of 0.601 indicates that the model has the precision model in moderate and can be accepted for predictive need.

The correlation coefficient (r) is 0.629, it indicates there is the strong enough relation between the prediction and observation values. Although this relation is not very strong, this value is keep reflecting the pattern consistency between the prediction result and actual data. However, the determination coefficient (R^2) is 0.396, it indicates that about 39.6% of variability on observation data can be explained by model. In other words, there is still about 60.4% of variability is not explained by model. It may be caused by the other factors outside the input variables or inaccuracy of model.

Based on the evaluation result above, the model development of flood risk assessment can be developed again by using linear regression modelling as follow:

$$R = a \cdot H^b \cdot C^d \cdot V^e \tag{1}$$

where a, b, d, e are regression coefficients. The model was linearized using natural logarithm transformation:

$$\ln(R) = \ln(a) + b \cdot \ln(H) + d \cdot \ln(C) + e \cdot \ln(V) \tag{2}$$

Systematically, the modelling result is presented in Table 3.

Table 3. Systematic of Modelling Result

Calculation Data				Modified Model with Linear Regression			
R	**H**	**C**	**V**	**Ln(R)**	**Ln(H)**	**Ln(C)**	**Ln(V)**
2.889	0.0810	9.635	7.537	1,061	-2.513	2.265	2.020
1.416	0.150	4.637	2.019	0,348	-1.897	1.534	0.703
3.065	0.323	7.547	3.910	1,120	-1.130	2.021	1.364
7.540	0.974	11.871	11.871	2,020	-0.026	2.474	2.474
12.377	3.165	44.601	26.496	2,516	1.152	3.798	3.277
12.945	0.064	22.910	15.972	2,561	-2.749	3.132	2.771
14.000	2.180	21.818	18.496	2,639	0.779	3.083	2.918
5.965	1.190	32.833	6.378	1,786	0.174	3.491	1.853
6.446	0.935	12.287	7.941	1,863	-0.067	2.509	2.072
5.969	0.557	15.047	7.169	1,787	-0.585	2.711	1.970
30.543	4.356	70.389	47.326	3,419	1.472	4.254	3.857

By using the function of LINEST on excel, so there is obtained the model coefficient as follows: a= 0.695, b= 0.032, d= 0.233, e= 0.711, so the formulation of flood risk assessment is as follows: $R = 0{,}695.H^{0.032}.\ C^{233}.\ V^{0{,}711}$. Performance evaluation of this model showed RMSE = 9.392, NSE = 0.756, $r = 0.793$, and $R^2 = 0.629$, demonstrating good predictive accuracy and strong consistency between predicted and observed values. While approximately 37% of variability remains unexplained, the model provides a robust basis for flood risk assessment and evidence-based disaster management.

To ensure that the flood risk assessment model is not overfitted, we conducted rigorous statistical validation beyond the use of R^2 by applying a training–testing split (80% training, 20% testing) and evaluating predictive performance using RMSE and NSE. In our analysis, the model achieved an RMSE of 5.748 and an NSE of 0.754 on the training subset, while on the testing subset it attained an RMSE of 5.765 and an NSE of 0.881. The negligible difference in RMSE between training and testing, combined with the higher NSE in testing, strongly suggests that the model possesses stable and generalizable performance, rather than being over-fitted to the calibration data.

This validation strategy parallels the principle of cross validation, which is widely recognized in hydrological modelling for its effectiveness in testing model robustness and preventing overfitting [21]. Indeed, NSE is a well-established metric for measuring hydrological model skill, and its use along with RMSE provides a balanced view of both bias and variability [22]. Furthermore, combining split sample validation with other statistical checks (such as hidden Markov modelling) has been demonstrated in the literature to enhance the robustness assessment of hydrological models [23].

While the linear regression model used in this study provides reliable flood risk predictions, it has inherent limitations due to the non-linear nature of hydrological processes. Validation using an 80%–20% training–testing split showed stable performance without overfitting, indicating that the model is suitable for flood risk assessment in the Juwana watershed.

Therefore, through this comprehensive validation framework, we provide statistical evidence that our flood risk model is not overfitted but rather reliably predictive, making it a sound basis for evidence-based disaster management and flood risk assessment. Overall, the log linear regression model is effective and feasible for practical application. Further refinements, including additional variables or nonlinear modelling approaches, can improve predictive accuracy for complex flood hazard scenarios.

4. Discussions

This study advances the understanding of spatially integrated flood risk assessment by developing an adaptive model that combines Geographic Information Systems (GIS) and Multi-Criteria Risk Assessment (MCRA) within a spatial planning framework [24]. The results demonstrate a strong correlation between urban expansion and the increasing frequency and intensity of floods. Areas experiencing rapid land use transformation—particularly from agricultural to urban functions—tend to exhibit higher flood vulnerability, reflected in deeper inundation, longer flood duration, and more frequent flood occurrences [23].

Traditionally, flood risk models have represented hazard (H) primarily through flood depth, emphasizing the extent of inundation while perhaps overlooking the potential destructive force of flowing water. In conventional models, R is often expressed as $H\cdot(V/C)$, where H represents the flood depth. It has been observed that areas with similar water levels may be assigned comparable risk, despite potential differences in the actual physical impact on infrastructure and property. Conversely, incorporating destructive power as H enables the model to capture both the intensity and potential for damage, thereby providing a more realistic assessment of flood consequences [24]. The empirical model ($R = 0.695\cdot H^{0.032}\cdot C^{0.233}\cdot V^{0.711}$) indicates that, in regions exposed to high destructive power, moderate levels of vulnerability or institutional capacity are insufficient to completely mitigate the elevated flood risk. This approach highlights the need to integrate hazard severity into flood risk assessment, enabling more effective management and prioritization of mitigation strategies.

The use of destructive power (H) as the hazard component in flood risk assessment highlights areas with the highest potential for physical damage, rather than simply the deepest water. This approach identifies zones where fast-moving or high-momentum floodwaters have the potential to cause significant harm to infrastructure, property, and human life. By focusing on these key areas, flood risk maps can become more realistic and actionable, offering a solid foundation for disaster preparedness [25].

The integration of destructive power (H) into the flood risk model enables the identification of strategic evacuation routes by explicitly considering areas with the highest potential physical impact. GIS-based spatial analysis is employed to map high-risk zones, determine evacuation starting points, and delineate routes that minimize exposure to high-destructive floodwaters. Evacuation paths are optimized according to criteria such as elevation, flow velocity, and infrastructure condition, prioritizing rapid access to safe shelters. This approach also facilitates efficient allocation of emergency resources, including medical posts and logistics distribution points, and supports risk-based evacuation scenarios that can be quantitatively tested prior to flood events. Consequently, evacuation planning is informed not only by geographical location but also by hazard intensity, thereby enhancing community safety and the operational effectiveness of emergency response [23, 24].

The findings of this study are broadly consistent with prior investigations in Indonesian and Southeast Asian watersheds, while also highlighting important distinctions. Studies by Apel et al. [7] and Pradhan et al. [9] primarily quantified flood risk using flood depth or population exposure, often neglecting the destructive power of floodwaters and institutional capacity. In contrast, the present model integrates destructive power (H) and institutional capacity (C) alongside vulnerability (V), providing a more comprehensive representation of flood risk dynamics.

Compared to other GIS-based MCRA studies in similar regions [26–28], the empirical calibration employed here allows improved spatial resolution and quantitative accuracy, particularly in capturing high-risk zones affected by rapid urban expansion and land-use change. Unlike prior studies that often focused solely on physical or socio-economic indicators, the current approach demonstrates how multi-dimensional risk factors interact, revealing areas where strong institutional capacity mitigates otherwise high vulnerability.

Spatial patterns observed in the Juwana watershed also show similarities with findings in the Ciliwung River Basin [29], where highly urbanized lowlands exhibit elevated flood risk due to high exposure and constrained cross-jurisdictional governance. By contrast, our study emphasizes the moderating role of institutional capacity more explicitly, akin to the adaptive capacity challenges identified in the Brantas River Basin [30], thereby providing more actionable insights for coordinated, policy-driven flood resilience planning."

5. Conclusion

This study demonstrates that incorporating destructive power (H), along with vulnerability (V) and institutional capacity (C), into flood risk assessment provides a more comprehensive and realistic representation of flood dynamics compared to traditional models based solely on flood depth. The empirical model developed here ($R = 0.695 \cdot H^{0.032} \cdot C^{0.233} \cdot V^{0.711}$) effectively identifies areas where moderate institutional capacity or vulnerability levels are insufficient to mitigate high flood risk, highlighting zones with the greatest potential for physical damage.

By integrating Geographic Information Systems (GIS) with Multi-Criteria Risk Assessment (MCRA), the study not only enhances the spatial resolution and quantitative accuracy of flood risk maps but also enables practical applications such as risk-informed evacuation planning and optimized allocation of emergency resources. The results underscore the critical interplay between rapid urbanization, land-use change, and institutional capacity in shaping flood vulnerability, providing actionable insights for disaster preparedness and policy-driven flood resilience strategies.

The findings collectively suggest that incorporating hazard strength, socio economic vulnerabilities, and governance capabilities into flood risk assessments creates a robust framework for managing floods and minimizing adverse effects on communities in fast developing watersheds.

6. Declarations

6.1. Author Contributions

Conceptualization, Y.A. and P.T.J.; methodology, Y.A.; validation, Y.A.; formal analysis, Y.A.; investigation, Y.A. and P.T.J.; resources, Y.A. and L.M.L.; data curation, Y.A. and R.H.; writing—original draft preparation, Y.A. and R.H.; writing—review and editing, L.M.L. and P.T.J.; visualization, Y.A. and R.H. All authors have read and agreed to the published version of the manuscript.

6.2. Data Availability Statement

The data presented in this study are available in the article.

6.3. Funding

The authors received no financial support for the research, authorship, and/or publication of this article.

6.4. Institutional Review Board Statement

Not applicable.

6.5. Informed Consent Statement

Not applicable.

6.6. Declaration of Competing Interest

The authors declare that there are no conflicts of interest concerning the publication of this manuscript. Furthermore, all ethical considerations, including plagiarism, informed consent, misconduct, data fabrication and/or falsification, double publication and/or submission, and redundancies have been completely observed by the authors.

7. References

[1] Franci, F., Mandanici, E., & Bitelli, G. (2015). Remote sensing analysis for flood risk management in urban sprawl contexts. Geomatics, Natural Hazards and Risk, 6(5-7), 583-599. doi:10.1080/19475705.2014.913695.

[2] Sun, Q., Fang, J., Dang, X., Xu, K., Fang, Y., Li, X., & Liu, M. (2022). Multi-scenario urban flood risk assessment by integrating future land use change models and hydrodynamic models. Natural Hazards and Earth System Sciences, 22(11), 3815–3829. doi:10.5194/nhess-22-3815-2022.

[3] Mustafa, A., Szydłowski, M., Veysipanah, M., & Hameed, H. M. (2023). GIS-based hydrodynamic modeling for urban flood mitigation in fast-growing regions: a case study of Erbil, Kurdistan Region of Iraq. Scientific Reports, 13(1), 8935. doi:10.1038/s41598-023-36138-9.

[4] Ahmad, I., Farooq, R., Ashraf, M., Waseem, M., & Shangguan, D. (2025). Improving flood hazard susceptibility assessment by integrating hydrodynamic modeling with remote sensing and ensemble machine learning. Natural Hazards, 1-30. doi:10.1007/s11069-025-07109-2.

[5] Motta, M., de Castro Neto, M., & Sarmento, P. (2021). A mixed approach for urban flood prediction using Machine Learning and GIS. International Journal of Disaster Risk Reduction, 56, 102154. doi:10.1016/j.ijdrr.2021.102154.

[6] Azadgar, A., Nyka, L., & Salata, S. (2024). Advancing urban flood resilience: A systematic review of urban flood risk mitigation model, research trends, and future directions. Land, 13(12), 2138. doi:10.3390/land13122138.

[7] Apel, H., Thieken, A. H., Merz, B., & Blöschl, G. (2004). Flood risk assessment and associated uncertainty. Natural Hazards and Earth System Science, 4(2), 295–308. doi:10.5194/nhess-4-295-2004.

[8] Mudashiru, R. B., Sabtu, N., Abustan, I., & Balogun, W. (2021). Flood hazard mapping methods: A review. Journal of Hydrology, 603, 126846. doi:10.1016/j.jhydrol.2021.126846.

[9] Pradhan, B., & Youssef, A. M. (2011). A 100-year maximum flood susceptibility mapping using integrated hydrological and hydrodynamic models: Kelantan River Corridor, Malaysia. Journal of Flood Risk Management, 4(3), 189-202. doi:10.1111/j.1753-318X.2011.01103.x.

[10] Maranzoni, A., D'Oria, M., & Rizzo, C. (2023). Quantitative flood hazard assessment methods: A review. Journal of Flood Risk Management, 16(1), e12855. doi:10.1111/jfr3.12855.

[11] Mojaddadi, H., Pradhan, B., Nampak, H., Ahmad, N., & Ghazali, A. H. B. (2017). Ensemble machine-learning-based geospatial approach for flood risk assessment using multi-sensor remote-sensing data and GIS. Geomatics, Natural Hazards and Risk, 8(2), 1080-1102. doi:10.1080/19475705.2017.1294113.

[12] Tanim, A. H., Goharian, E., & Moradkhani, H. (2022). Integrated socio-environmental vulnerability assessment of coastal hazards using data-driven and multi-criteria analysis approaches. Scientific Reports, 12(1), 11625. doi:10.1038/s41598-022-15237-z.

[13] Yoon, S. K., Kim, J. S., & Moon, Y. I. (2014). Integrated flood risk analysis in a changing climate: A case study from the Korean Han River Basin. KSCE Journal of Civil Engineering, 18(5), 1563-1571. doi:10.1007/s12205-014-0147-5.

[14] Collet, L., Beevers, L., & Stewart, M. D. (2018). Decision-making and flood risk uncertainty: Statistical data set analysis for flood risk assessment. Water Resources Research, 54(10), 7291-7308. doi:10.1029/2017WR022024.

[15] Rai, S. P., Young, W., & Sharma, N. (2017). Risk and opportunity assessment for water cooperation in transboundary river basins in South Asia. Water Resources Management, 31(7), 2187-2205. doi:10.1007/s11269-017-1637-2.

[16] Rizwan, M., Li, X., Chen, Y., Anjum, L., Hamid, S., Yamin, M., ... & Mehmood, Q. (2023). Simulating future flood risks under climate change in the source region of the Indus River. Journal of Flood risk management, 16(1), e12857. doi:10.1111/jfr3.12857.

[17] Franci, F., Bitelli, G., Mandanici, E., Hadjimitsis, D., & Agapiou, A. (2016). Satellite remote sensing and GIS-based multi-criteria analysis for flood hazard mapping. Natural Hazards, 83(Suppl 1), 31-51. doi:10.1007/s11069-016-2504-9.

[18] Feizizadeh, B., Gheshlaghi, H. A., & Bui, D. T. (2021). An integrated approach of GIS and hybrid intelligence techniques applied for flood risk modeling. Journal of Environmental Planning and Management, 64(3), 485-516. doi:10.1080/09640568.2020.1775561.

[19] Lin, L., Wu, Z., & Liang, Q. (2019). Urban flood susceptibility analysis using a GIS-based multi-criteria analysis framework. Natural Hazards, 97(2), 455-475. doi:10.1007/s11069-019-03615-2.

[20] Aroca-Jiménez, E., Bodoque, J. M., & García, J. A. (2020). How to construct and validate an Integrated Socio-Economic Vulnerability Index: Implementation at regional scale in urban areas prone to flash flooding. Science of the Total Environment, 746, 140905. doi:10.1016/j.scitotenv.2020.140905.

[21] El Garnaoui, M., Boudhar, A., Nifa, K., El Jabiri, Y., Karaoui, I., El Aloui, A., Midaoui, A., Karroum, M., Mosaid, H., & Chehbouni, A. (2024). Nested Cross-Validation for HBV Conceptual Rainfall–Runoff Model Spatial Stability Analysis in a Semi-Arid Context. Remote Sensing, 16(20), 3756. doi:10.3390/rs16203756.

[22] Guilpart, E., Espanmanesh, V., Tilmant, A., & Anctil, F. (2021). Combining split-sample testing and hidden Markov modelling to assess the robustness of hydrological models. Hydrology and Earth System Sciences, 25(8), 4611–4629. doi:10.5194/hess-25-4611-2021.

[23] Cançado, V., Brasil, L., Nascimento, N., & Guerra, A. (2008). Flood risk assessment in an urban area: Measuring hazard and vulnerability. Proceedings of the 11th International Conference on Urban Drainage, Edinburgh, Scotland, United Kingdom.

[24] Tabasi, N., Fereshtehpour, M., & Roghani, B. (2025). A review of flood risk assessment frameworks and the development of hierarchical structures for risk components. Discover Water, 5(1), 21. doi:10.1007/s43832-025-00193-2.

[25] Ricciardi, G., Ellena, M., Barbato, G., Alcaras, E., Parente, C., Carcasi, G., ... & Mercogliano, P. (2024). Risk assessment of national railway infrastructure due to sea-level rise: an application of a methodological framework in Italian coastal railways. Environmental Monitoring and Assessment, 196(9), 822. doi:10.1007/s10661-024-12942-2.

[26] Lasaiba, M. A., & Leuwol, F. S. (2024). Multi-Criteria Based Flood Hazard and Risk Analysis in Sirimau District, Ambon City. Spatial Journal of Geographical Communication and Information Technology, 24(2), 100–114. doi:10.21009/10.21009/spatial.242.001. (In Indonesian).

[27] Purwanto, A., Rustam, Eviliyanto, & Andrasmoro, D. (2022). Flood Risk Mapping Using GIS and Multi-Criteria Analysis at Nanga Pinoh West Kalimantan Area. Indonesian Journal of Geography, 54(3), 463–470. doi:10.22146/IJG.69879.

[28] Alyudin, D. R., Manessa, M. D. M., Purwaningsih, Y., & Yuningsih, Y. (2024). Spatial Analysis of Flood Vulnerability Using the Spatial Multi-Criteria Analysis Method in Ciputri Village, West Java. Geodika: Journal of Geographical Science and Education Studies, 8(2), 210-221. doi:10.29408/geodika.v8i2.27097.

[29] Rahayu, H. P., Zulfa, K. I., Nurhasanah, D., Haigh, R., Amaratunga, D., & Wahdiny, I. I. (2024). Unveiling transboundary challenges in river flood risk management: Learning from the Ciliwung River basin. Natural Hazards and Earth System Sciences, 24(6), 2045–2064. doi:10.5194/nhess-24-2045-2024.

[30] Prihanto, D., Rachmansyah, A., & Riniwati, H. (2019). Adaptive Capacity of Brantas Watershed in Malang City Fancing of the Climate Change Impact. Jurnal Pembangunan Dan Alam Lestari, 10(1), 5. doi:10.21776/ub.jpal.2019.010.01.05.